

Phonon Dispersion in Graphite

J. Maultzsch,¹ S. Reich,^{2,1} C. Thomsen,¹ H. Requardt,³ and P. Ordejón²

¹*Institut für Festkörperphysik, Technische Universität Berlin, Hardenbergstrasse 36, 10623 Berlin, Germany*

²*Institut de Ciència de Materials de Barcelona (CSIC), Campus de la U.A.B., 08193 Bellaterra, Spain*

³*European Synchrotron Radiation Facility (ESRF), B.P. 220, 38043 Grenoble, France*

(Received 11 September 2003; published 17 February 2004)

We measured the dispersion of the graphite optical phonons in the in-plane Brillouin zone by inelastic x-ray scattering. The longitudinal and transverse optical branches cross along the Γ - K as well as the Γ - M direction. The dispersion of the optical phonons was, in general, stronger than expected from the literature. At the K point the transverse optical mode has a minimum and is only ≈ 70 cm^{-1} higher in frequency than the longitudinal mode. We show that first-principles calculations describe very well the vibrational properties of graphene once the long-range character of the dynamical matrix is taken into account.

DOI: 10.1103/PhysRevLett.92.075501

PACS numbers: 63.20.Dj, 63.10.+a, 71.15.Mb, 78.70.Ck

Over the past few decades, a detailed knowledge of the optical, electronic, and vibrational properties of many solids has been obtained. For technologically important materials such as Si or GaAs this knowledge is comprehensive in common belief, and, naturally, one would expect graphite to belong to this group. Surprisingly, this is not the case regarding its vibrational properties. The modes below 400 cm^{-1} were measured by inelastic neutron scattering [1]. In the range of the optical modes (up to 1600 cm^{-1}) experiments are scarce [2–4]; the existing data scatter widely and are missing completely for the K - M symmetry direction. The dispersion of the transverse optical phonon is hardly known away from the Γ point; some experimental approaches involved complex calculations like double-resonant Raman scattering [5,6]. On the other hand, there are numerous findings that electron–optical-phonon and electron–electron interactions in sp^2 carbon is particularly strong at certain high-symmetry points. This was first noticed in connection with disorder-induced double-resonant Raman scattering in graphite as well as in carbon nanotubes [5–8]. Later, a Γ -point phonon softening by electron–phonon interaction in metallic nanotubes was reported [9], and, most recently, a renormalization of the electronic states by resonant electron–electron interaction [10]. Thus, the optical phonons play an important role in the free-carrier dynamics in graphite and carbon nanotubes as well as in the electronic transport in the high-voltage regime [11].

The absence of experiments on the high-energy phonons—which is mainly caused by the lack of large enough graphite single crystals—would be less disturbing if the dispersion was well established from a theoretical point of view. Unfortunately, existing calculations contradict each other qualitatively and quantitatively in frequencies, slopes, and crossings of particular phonon branches. For example, according to most of the calculations the transverse optical branch has a minimum at the K point [7,9,12,13], whereas others predict a local

maximum [6,14]. The calculated frequencies at the K and M point differ by up to 300 cm^{-1} , resulting in large differences in the slopes and even the general shape of the calculated phonon dispersions. An accurate measurement of the optical phonons is urgently called for to resolve these contradictions and establish the phonon dispersion of graphite, a basic property of any solid.

In this work we present the high-energy phonon branches of graphite along all high-symmetry directions in the in-plane Brillouin zone, i.e., along Γ - M , Γ - K , and K - M . Using inelastic x-ray scattering, we found the dispersion of the optical modes to be much stronger than assumed up to now. The bandwidth of the TO branch, for example, is 320 cm^{-1} , which is $\approx 40\%$ larger than in the most recent *ab initio* work [9]. Our data show that the LO and TO branches cross along the Γ - K and the Γ - M direction invalidating some of the existing force-constants calculations. Our *ab initio* calculations of the phonon dispersion agree well with the experiment. Previous deviations of first-principles calculations arose mostly from the assumption that the dynamical matrix is short ranged in this material.

The experiment was performed at the beam line ID28 at the European Synchrotron Radiation Facility [15–17]. We used an incident x-ray beam of $17\,794$ eV selected by a double-crystal Si(111) premonochromator. The high resolution in energy of 3.1 meV was obtained by the Si(999) backscattering reflection of the main monochromator. The combination of a cylindrical mirror (vertical focus) and an actively bent multilayer element (horizontal focus) provided a beam spot size of 30×60 μm^2 . The small focal spot allowed us to select a microcrystal (100×200 μm^2) in a naturally grown graphite flake. The scattering plane was perpendicular to the c axis. The momentum transfer Q was selected by the scattering angle of the 7 m long spectrometer arm with a set of five analyzers allowing the simultaneous detection at five different Q . The phonon wave vector q is determined

from the scattering vector $\mathbf{Q} = \mathbf{q} + \mathbf{H}$, where \mathbf{H} is a reciprocal lattice vector. The incident photon energy was scanned by changing the temperature of the main monochromator.

Symmetry-imposed selection rules for inelastic x-ray scattering are particularly strict in the D_{6h}^4 space group of graphite. They apply in addition to the standard rule that only those phonons are observable whose polarization possesses a component along \mathbf{Q} . For phonon eigenvectors determined by symmetry alone, the general selection rules contain the polarization rule. The selection rules, which are important for the identification of the observed peaks, can be derived as described by Perez-Mato *et al.* [18,19]. For example, if $\mathbf{q} \parallel \mathbf{Q}$, the fully symmetric modes are always allowed. To measure the LO branch along Γ - K (B_1 symmetry in C_{2v}), we had to use $\mathbf{H} = (100)$ so that the polarization of the phonon was not parallel to \mathbf{Q} [Fig. 1(a)]. In contrast, for $\mathbf{H} = (2\bar{1}0)$ and \mathbf{q} along Γ - K , the LO mode is forbidden. In this direction, the TO branch possesses the allowed A_1 symmetry but has a large polarization component perpendicular to \mathbf{Q} . Close to the K point, the phonons lose their purely longitudinal or transverse character and the TO phonon is observed; see Fig. 1(b). For simplicity we use the terms LO and TO in the entire Brillouin zone for the in-plane phonon branches which are strictly longitudinal and transverse only at the Γ point.

The full dots in Fig. 2 show the phonon dispersion of graphite measured by inelastic x-ray scattering; Table I lists the frequencies at high-symmetry points. The Γ point frequency is in good agreement with Raman measurements on a single crystal of graphite (1575 cm^{-1}) [20], which is slightly lower than the 1582 cm^{-1} reported on highly oriented pyrolytic graphite. The LO branch exhibits an overbending of 30 cm^{-1} in both high-symmetry directions. After its maximum at $q \approx 0.15H = 0.15(4\pi/\sqrt{3}a_0)$ the dispersion bends down much stronger than previously believed. At the K point the E' mode is at 1194 cm^{-1} , whereas in the literature it is usually placed between 1240 and 1500 cm^{-1} [6,9]. At the

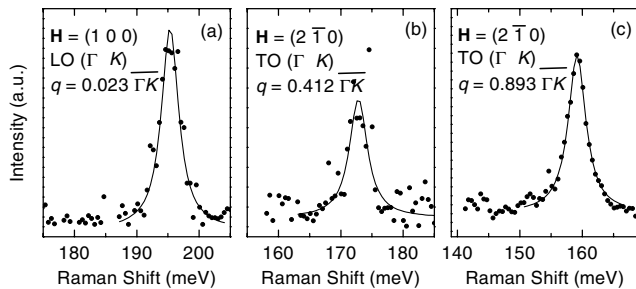


FIG. 1. Inelastic x-ray spectra of graphite along Γ - K ; q is in units of the distance between Γ and K . (a) The LO phonon along Γ - K is observed if \mathbf{q} and \mathbf{Q} are not parallel, e.g., if $\mathbf{H} = (100)$. (b),(c) Along Γ - K with $\mathbf{H} = (2\bar{1}0)$ ($\mathbf{q} \parallel \mathbf{Q}$), the TO mode is allowed (A_1 symmetry). It is observed only at large q , where it has a polarization component parallel to $\mathbf{Q} = \mathbf{H} + \mathbf{q}$.

M point the longitudinal optical and acoustic phonon are at 1323 and 1290 cm^{-1} , respectively. The latter branch is in very good agreement with electron-energy-loss spectroscopy measurements [3]. The common underestimation of the dispersion strength is even more pronounced for the transverse optical phonon.

At the K point the TO was believed to have an energy above 1350 cm^{-1} . In contrast to this expectation we obtained a frequency of $1265 \pm 10 \text{ cm}^{-1}$ from an extrapolation of our x-ray measurements (dashed line in Fig. 2). Directly at the K point A_1' scattering was either forbidden by selection rules or the mixed LO-TO character of the mode made the scattering intensity too weak for observation. Nevertheless, the measured TO frequencies close to the K point are well below 1300 cm^{-1} ; see Figs. 2 and 1(c).

The A_1' (TO) phonon frequency at K is thus rather close to the previously predicted E' (LO) energies, which resolves a contradiction in the interpretation of the Raman data in graphite. The solid-state picture of double-resonant scattering argued that the LO branch is responsible for the D mode in the Raman spectra of graphite, because the absolute frequencies and the calculated excitation-energy dependence agreed well with experiment [5]. On the other hand, from their studies on small aromatic molecules, Mapelli *et al.* [7] found the totally symmetric mode to have a strong Raman signal, which pointed at the A_1' phonon branch of graphite [21]. It seems that this discrepancy can be resolved using the correct phonon dispersion in the calculations of double-resonant Raman spectra [22].

For the calculations of the vibrational properties of graphene, i.e., a single sheet of graphite, we used the SIESTA package [23]. Because of the weak interaction between the graphene layers, the high-energy phonons of graphite have approximately the same frequency as in graphene and are doubly degenerate [9]. The core electrons were replaced by pseudopotentials [24]; the valence electrons were described by localized pseudoatomic orbitals [25]. We tested the convergence of the *ab initio* results with respect to the exchange and correlation functional, basis set completeness, and k -point sampling by frozen phonon calculations. We also included features such as Methfessel smearing or an additional sampling in real space to remove the so-called egg-box effect, but found the phonon frequencies rather insensitive to these additives; a detailed report will be published elsewhere. Instead of the first-order local density functional approximation (LDA) we used the generalized gradient approximation (GGA) as parametrized by Perdew *et al.* [26]. The valence electrons were described by a double- ζ polarized basis set with a cutoff radius of 5.00 a.u. for the s and 6.25 a.u. for the p and the polarizing d orbital [25]. The mesh cutoff in real space was 320 Ry ; we used more than 3300 k points for the graphene unit cell. We calculated the force constants by finite differences for stripes of graphene which allowed a description

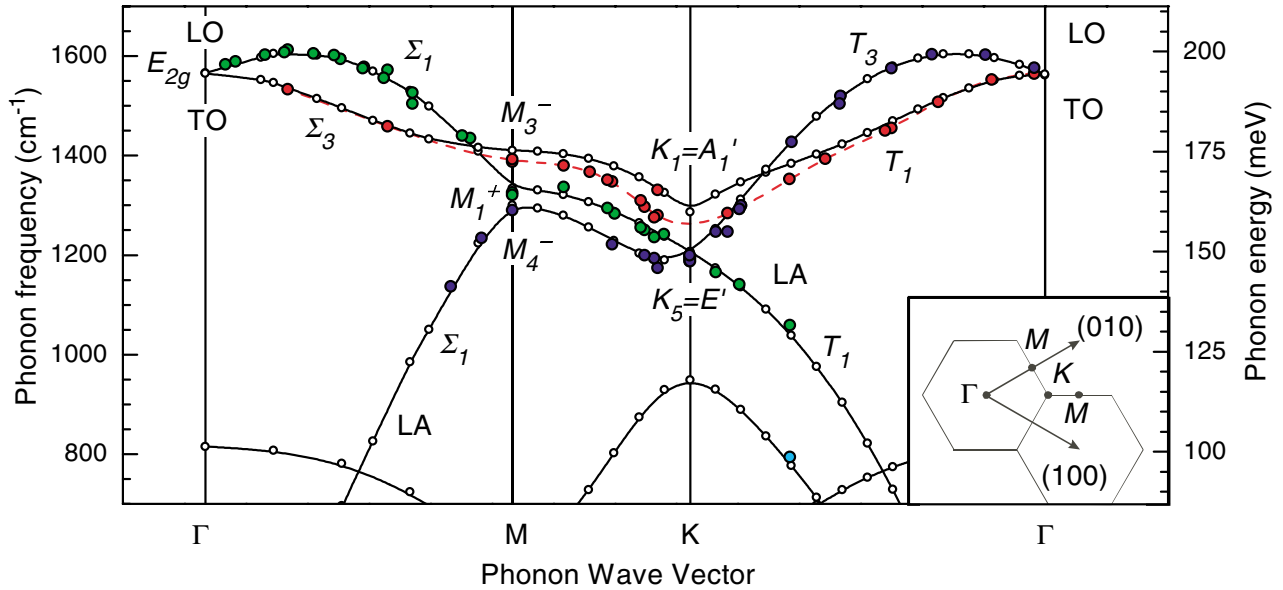


FIG. 2 (color online). Inelastic x-ray scattering and *ab initio* calculations of the phonon dispersion of graphite. The symmetry of the branches is indicated; see Table I. Filled dots are the experimental data for the LO, TO, and the LA branch. The TO data are connected by a cubic spline extrapolation (dashed line). The experimental error is smaller than the size of the symbols. Those phonon wave vectors \mathbf{q} , which were not exactly along the Γ - M or Γ - K - M direction, were projected onto the closest high-symmetry direction. Open dots are the calculated phonon frequencies; they were scaled overall by 1% to smaller frequencies. The lines are a spline extrapolation to the calculated points. Inset: Brillouin zone of graphite in the basal plane with the high-symmetry points Γ , K , and M . The arrows indicate the reciprocal lattice vectors with magnitude $H = |\mathbf{H}| = 4\pi/(\sqrt{3}a_0)$, where a_0 is the in-plane lattice constant of graphite.

of modes propagating along the high-symmetry directions. For Γ - K - M we used a supercell with 84 atoms, for Γ - M 18 and 22 atoms in two different calculations.

In Fig. 2 we show by open dots the graphene frequencies calculated from first principles; they are scaled by 1% to smaller frequencies. For the longitudinal branches the agreement between theory and experiment is excellent. The overbending, the small splitting of the LO and LA at the M point (30 cm^{-1} ; see Table I), and the local minimum of the lowest B_1 branch between K and M (1185 cm^{-1}) are very well described by the first-principles results. A good agreement for the TO is found along the Γ - M direction. Along Γ - K - M the *ab initio* dispersion is slightly less pronounced than the experimen-

tal result. Our calculated splitting between the A'_1 and the E' mode at K (80 cm^{-1}), however, is quite close to the measured splitting of 70 cm^{-1} , whereas in previous work an LDA result of 140 cm^{-1} was reported [9]. Similarly, Pavone *et al.* [12] obtained a splitting of 120 cm^{-1} , although at the other high-symmetry points their results agree well with the experiments. The better agreement of the *ab initio* calculations presented here with experiment as compared to published work is only partly due to the GGA. More important is that the dynamical matrix in (semi)metals like graphene is not short ranged as it is in semiconductors. The correct frequencies and eigenvectors can thus be found only for phonons commensurate with the supercell used in the force-constants calculations

TABLE I. Frequencies at the high-symmetry points of the Brillouin zone. The phonon symmetry is given by two notations; the second is the molecular notation. The graphite point group D_{6h} reduces to C_{2v} between the high-symmetry points, and to D_{3h} and D_{2h} at the K and the M point, respectively. In the last two columns the overbending $\Delta\omega$, i.e., the difference between the maximum and the Γ -point frequency, of the LO branch is given. q_{\max} denotes the wave vector at the maximum frequency in units of the reciprocal lattice vector. The experimental error of most frequencies is below 2 meV. The calculated frequencies are not scaled.

	TO (cm^{-1})		LO (cm^{-1})		LA (cm^{-1})		q_{\max} ($4\pi/\sqrt{3}a_0$)		$\Delta\omega$ (cm^{-1})								
	exp	theo	sym	exp	theo	sym	exp	theo	exp	theo							
Γ (Γ - M)		1581	Σ_3	B_1	1583	1582	Σ_1	A_1									
Γ (Γ - K)	1565	1581	T_1	A_1	1577	1581	T_3	B_1			0	T_1	A_1	0.15	0.15	30 ± 5	36
M	1390	1425	M_3^-	B_{2u}	1323	1350	M_1^+	A_g	1290	1315	M_4^-	B_{3u}					
K	1265 ^a	1300	K_1	A'_1	1194	1220	K_5	E'	1194	1220	K_5	E'					

^aObtained from a spline extrapolation of the data.

(open dots in Fig. 2). The error in frequency if not taking this into account is most pronounced for the A'_1 mode at K ($\approx 50 \text{ cm}^{-1}$) while the E' mode and the M point frequencies are affected much less ($\approx 10\text{--}35 \text{ cm}^{-1}$).

Dubay *et al.* [9] recently predicted a phonon softening in metallic carbon nanotubes, which was mediated by a strong electron-phonon coupling of the graphenelike Γ -point mode to the π electronic bands. This effect can be mimicked in graphene by using a sparse k -point sampling in the phonon calculation. The Γ -point frequency then rapidly drops to 1500 cm^{-1} and below. We observed, however, an even stronger softening for the A'_1 mode at K , which couples the π bands at two different K points in the Brillouin zone. We suggest also in carbon nanotubes a softening similar to that at the Γ point for the modes corresponding to the graphene K point. Raman measurements indicate that this is indeed the case: First, the D mode in single-walled carbon nanotubes is usually $\approx 20 \text{ cm}^{-1}$ lower than in graphite at the same excitation energy [8,27]. Second, a linear extrapolation of the D mode frequencies to zero excitation energy, i.e., a lower bound to the K point frequency, yields 1245 cm^{-1} in graphite, in reasonable agreement with our x-ray measurements. For an isolated metallic nanotube, however, the same procedure leads to a frequency of 1190 cm^{-1} [8]. The strong electron-phonon coupling for the K point optical modes also explains the current saturation in high-voltage transport measurements observed by Yao *et al.* [11]. They suggested that scattering by phonons with an energy $\approx 1300 \text{ cm}^{-1}$ gives rise to the dramatic conductance drop at high bias. Again this energy matches well with the A'_1 phonon energy. Finally, the softening of the Γ and K point optical phonons also explains the discrepancies between the graphene dispersion calculated by Mapelli *et al.* [7] and other *ab initio* work. Mapelli *et al.*, in a molecular approach, used the force field they obtained from first principles for small aromatic molecules to calculate the properties of graphene. Because of the softening expected for small graphenelike molecules, they obtained the K point A'_1 (1260 cm^{-1}) energy very close to the experimental results, underestimating, however, the frequencies at other points (e.g., 1554 cm^{-1} at Γ).

In conclusion, we determined the high-energy phonon dispersion of graphite in all high-symmetry directions of the in-plane Brillouin zone. Using inelastic x-ray measurements and first-principles calculations we established a coherent description of the vibrational properties of this material. We found that the dispersion of the optical phonons was usually underestimated in the past, in particular, for the transverse optical branch along Γ - K - M . We showed that the discrepancies in previous theoretical work arose from the long-range nature of the in-plane force constants of graphite. Our work resolves contradictions such as the assignment of the D mode in graphite. We confirmed that the E_{2g} Γ point and the A'_1 K -point

phonon couple very strongly to the electronic bands in sp^2 bonded carbon. Since the properties of graphite are the basis for a large number of other materials such as carbon nanotubes or intercalated graphite, our findings can guide further work in both theory and experiment.

We are indebted to A.V. Tamashauskyy for the rare single crystals of graphite. We thank X. Blase and D. Sánchez-Portal for helpful discussions on the phonon calculations, S. Morgner for a Raman characterization of the sample, and A. Krost, K. Schatke, and U. Pohl for the Laue characterization. S.R. acknowledges a support by the Berlin-Brandenburgische Akademie der Wissenschaften. This work was supported by the Deutsche Forschungsgemeinschaft under Grant No. Th662/8-2 and by the ESRF. The calculations were performed on the CESCA and CEPBA supercomputing facilities.

-
- [1] R. Nicklow, N. Wakabayashi, and H.G. Smith, *Phys. Rev. B* **5**, 4951 (1972).
 - [2] J.L. Wilkes, R.E. Palmer, and R.F. Willis, *J. Electron Spectrosc. Relat. Phenom.* **44**, 355 (1987).
 - [3] C. Oshima *et al.*, *Solid State Commun.* **65**, 1601 (1988).
 - [4] S. Siebentritt, R. Poes, and K.-H. Rieder, *Phys. Rev. B* **55**, 7927 (1997).
 - [5] C. Thomsen and S. Reich, *Phys. Rev. Lett.* **85**, 5214 (2000).
 - [6] R. Saito *et al.*, *Phys. Rev. Lett.* **88**, 027401 (2002).
 - [7] C. Mapelli *et al.*, *Phys. Rev. B* **60**, 12 710 (1999).
 - [8] J. Maultzsch *et al.*, *Phys. Rev. Lett.* **91**, 087402 (2003).
 - [9] O. Dubay and G. Kresse, *Phys. Rev. B* **67**, 035401 (2003).
 - [10] C.L. Kane and E.J. Mele, *Phys. Rev. Lett.* **90**, 207401 (2003).
 - [11] Z. Yao, C.L. Kane, and C. Dekker, *Phys. Rev. Lett.* **84**, 2941 (2000).
 - [12] P. Pavone *et al.*, *Physica (Amsterdam)* **220B**, 439 (1996).
 - [13] D. Sánchez-Portal *et al.*, *Phys. Rev. B* **59**, 12 678 (1999).
 - [14] R.A. Jishi and G. Dresselhaus, *Phys. Rev. B* **26**, 4514 (1982).
 - [15] F. Sette *et al.*, *Phys. Rev. Lett.* **75**, 850 (1995).
 - [16] T. Ruf *et al.*, *Phys. Rev. Lett.* **86**, 906 (2001).
 - [17] J. Kulda *et al.*, *Phys. Rev. B* **66**, 241202 (2002).
 - [18] J.M. Perez-Mato *et al.*, *Phys. Rev. Lett.* **81**, 2462 (1998).
 - [19] A.K. Kirov, M.I. Aroyo, and J.M. Perez-Mato, *J. Appl. Crystallogr.* **36**, 1085 (2003).
 - [20] F. Tuinstra and J.L. Koenig, *J. Chem. Phys.* **53**, 1126 (1970).
 - [21] A. Ferrari and J. Robertson, *Phys. Rev. B* **61**, 14 095 (2000).
 - [22] J. Maultzsch, S. Reich, and C. Thomsen (to be published).
 - [23] J.M. Soler *et al.*, *J. Phys. Condens. Matter* **14**, 2745 (2002).
 - [24] N. Troullier and J.L. Martins, *Phys. Rev. B* **43**, 1993 (1991).
 - [25] J. Junquera *et al.*, *Phys. Rev. B* **64**, 235111 (2001).
 - [26] J.P. Perdew, K. Burke, and M. Ernzerhof, *Phys. Rev. Lett.* **77**, 3865 (1996).
 - [27] S.D.M. Brown *et al.*, *Phys. Rev. B* **64**, 073403 (2001).